

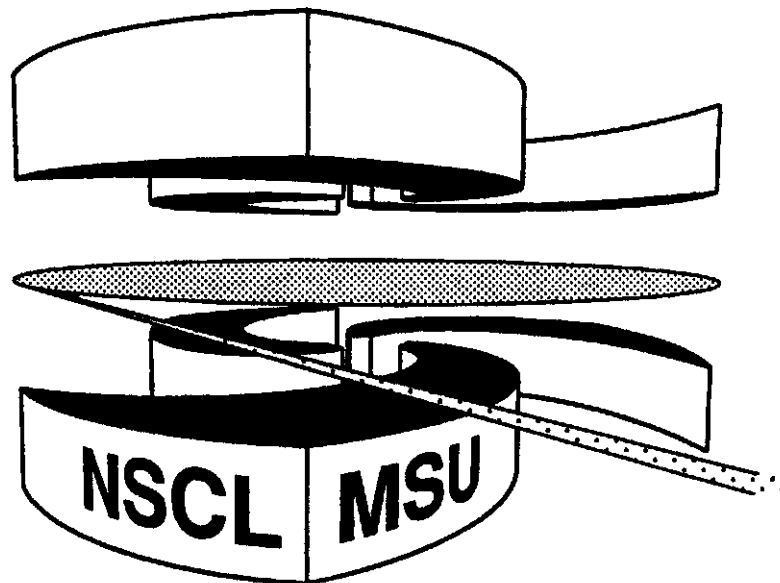


Michigan State University

National Superconducting Cyclotron Laboratory

DYNAMICAL EMISSION AND ISOTOPE THERMOMETRY

**H. XI, G.J. KUNDE, O. BJARKI, C.K. GELBKE,
R.C. LEMMON, W.G. LYNCH, D. MAGESTRO,
R. POPESCU, R. SHOMIN, M.B. TSANG,
A.M. VANDER MOLEN, G.D. WESTFALL, G. IMME,
V. MADDALENA, C. NOCIFORO, G. RACITI,
G. RICCOBENE, F.P. ROMANO, A. SAIJA, C. SFIENTI,
S. FRITZ, C. GROB, T. ODEH, C. SCHWARZ,
A. NADASEN, D. SISAN, K.A.G. RAO**



Dynamical Emission and Isotope Thermometry

H.F. Xi, G. J.Kunde¹, O. Bjarki, C.K. Gelbke, R.C. Lemmon², W.G. Lynch, D. Magestro, R. Popescus, R.Shomin, M.B. Tsang, A.M. Vander Molen, G.D. Westfall

Department of Physics and Astronomy and National Superconducting Cyclotron Laboratory, Michigan State University, East Lansing, MI 48824, USA,

G. Imme, V. Maddalena, C. Nociforo, G. Raciti, G. Riccobene, F.P. Romano, A. Saija, C. Sfienti,

Dipartimento di Fisica Università and I.N.F.N. Sezione and Laboratorio Nazionale del SUD - Catania, 195127, Catania, Italy

S. Fritz, C. Groß, T. Odeh, C. Schwarz

Gesellschaft für Schwerionenforschung, D-64220 Darmstadt, Germany,

A. Nadasen, D. Sisan, K.A.G. Rao

Department of Natural Sciences, University of Michigan, Dearborn, MI 48128, USA

Abstract

Ratios of the populations of ground and excited states of ^4He , ^5Li , and ^8Be and double ratios constructed from the yields $^3,^4\text{He}$, $^6,^7,^8\text{Li}$, $^{11,12,13}\text{C}$ isotopes were measured for central Kr+Nb collisions at $E/A=35, 70, 100,$ and 120 MeV . These ratios were analyzed to estimate an apparent temperature for emission. Consistent and approximately constant apparent temperatures were obtained from the excited states of ^4He , ^5Li , and ^8Be nuclei and from thermometers based upon the yields of carbon isotopes. In contrast, apparent temperatures obtained from thermometers based upon the ratios using helium isotopes increase monotonically with incident energy.

¹Present address: Yale University, New Haven CT 06520, U.S.A.

²Present address: CCLRC, Daresbury Laboratory, Daresbury, Cheshire WA44AD, U.K.

³ Present address: Brookhaven National Laboratory, Upton, NY 11973, U.S.A.

One of the general expectations for a system undergoing a first order phase transition is an enhanced heat capacity at temperatures where the phase transition occurs, reflecting the latent heat required to transform from one phase to the other. Calculations predict enhanced heat capacities for finite nuclear systems at temperatures of the order of 4-6 MeV [1-3], due to the transformation from the Fermi liquid which can be found in the interior of large nuclei in their ground and low excited states to a gas phase consisting of free nucleons and light clusters[3]. Temperatures extracted from the isotopic abundances of helium and lithium fragments [4] produced by the fragmentation of Au projectiles [5] display a “caloric curve” consistent with the hypothesis of a mixed phase equilibrium. These results have stimulated a large body of experimental [5-12] and theoretical [13-17] work, both supportive and critical of the caloric and thermometric techniques employed.

To reduce the sensitivity to collective motion [18], temperatures for hot nuclear systems formed in nucleus-nucleus collisions have been extracted from the comparison of ratios of isotopic yields, T_{iso} [5-12], and excited state populations, $T_{\Delta E}$ [7,12,19-24]. For thermal distributions at low density and at chemical equilibrium, prior to the secondary decay of the excited fragments, the double ratios R_{iso} of the ground state yields of four suitably chosen isotopes are given by [4]:

$$R_{iso} = \frac{Y(A_1, Z_1) / Y(A_1 + 1, Z_1)}{Y(A_2, Z_2) / Y(A_2 + 1, Z_2)} = \frac{1}{a} \exp(B / T) \quad (1)$$

where $Y(A_i, Z_i)$ is the yield for isotope with mass A_i and charge Z_i ; a is a statistical factor determined by spin values and kinematics factors; $B = BE(A_1, Z_1) - BE(A_1 + 1, Z_1) - BE(A_2, Z_2) + BE(A_2 + 1, Z_2)$; and $BE(A_i, Z_i)$ is the binding energy of the i^{th} nucleus. Such double yield ratios have the advantage of being insensitive to chemical potential terms which strongly influence the fragment isotopic distributions [4].

Similarly, the ratios R_{ij} of the yields of states i and j of a specific fragment, prior to the secondary decay of the excited fragments, are given by [26]:

$$R_{ij} = \frac{Y_i}{Y_j} = \frac{(2J_i + 1)}{(2J_j + 1)} e^{-(E_i^* - E_j^*)/T} \quad (2)$$

where Y_i is the yield, E_i^* is the excitation energy, and J_i is the spin of the state i . In the context of rate equation approaches [27], instantaneous particle emission rates depend upon instantaneous temperatures in ways analogous to Eqs. (1) and (2); however, the total yields reflect an averaging over the time dependent cooling of the system [28-30]. “Apparent” temperatures obtained from Eqs. (1) or (2), often require corrections for the secondary decay of excited fragments. The exact magnitude of such corrections depends on the isotope or excited state ratio and the temperature [7,11,13,14]. These corrections can be minimized by choosing ratios characterized by large binding energy differences B in Eq. (1) or large $\Delta E = E_i^* - E_j^*$ in Eq. (2) (i.e. $B, \Delta E \gg T$).

Consistent values of T_{iso} and $T_{\Delta E}$ for large B and ΔE , respectively, have been obtained for central Au+Au collisions at incident energies $35 \text{ MeV} \leq E/A \leq 50 \text{ MeV}$ [7,12]. For $E/A > 50 \text{ MeV}$, however, temperatures from the two methods diverge: values for $T_{iso}(He)$ extracted from Eq. (1) using yields of 3He and 4He isotopes increase with incident energy but values for $T_{\Delta E}$ extracted from Eq. (2) using yields of highly excited states of 4He , 5Li and 8Be nuclei do not [12]. This discrepancy has been argued to be the result of a suppression of the numbers of highly excited fragments within the disintegrating nuclear medium [14] which would lower the values of $T_{\Delta E}$ extracted via Eq. (2). Alternatively, early emission of 3He [28, 30] could elevate the $^3He/^4He$ isotopic ratio and raise the values of $T_{iso}(He)$ extracted via Eq. (1). In this paper, we determine T_{iso} and $T_{\Delta E}$ for central Kr+Nb collisions at $E/A=35, 70, 100$ and 120 MeV . Values of T_{iso} are extracted both from $Y(^3He)/Y(^4He)$ and from $Y(^{11}C)/Y(^{12}C)$ ratios -- both of which have large B values [6,13]. Consistent with the findings for Au+Au collisions, $T_{iso}(He)$ and $T_{\Delta E}$ agree at low energies ($E/A=35 \text{ MeV}$) but disagree at higher energies. Surprisingly, our results show that $T_{iso}(C)$ from carbon isotopes agree with $T_{\Delta E}$ from excited states. Thus, non-statistical 3He emission maybe a more likely explanation of the discrepancy between $T_{iso}(He)$ and $T_{\Delta E}$ values than the suppression of excited fragments within the disintegrating nuclear medium.

The experiment was performed by bombarding ^{93}Nb targets of 6 and 20 mg/cm^2 areal density with ^{86}Kr beams at $E/A=35, 70, 100, 120$ MeV from the National Superconducting Cyclotron Laboratory at Michigan State University (MSU). Impact parameters were selected by gates on the multiplicity of identified charged particles detected at polar angles of $\theta_{\text{lab}} = 7^\circ\text{-}157^\circ$ using 215 plastic ΔE - E phoswich detectors of the MSU 4π Array. The data presented here represent central collisions with a charged particle multiplicity selection on the MSU 4π array corresponding to the top 20% of the total cross section and reduced impact parameter $b/b_{\text{max}} \leq 0.45$.

Two hexagonal modules of the 4π array, located at $\theta_{\text{lab}} = 37^\circ$ and 79° were replaced by a 96-telescope hodoscope (HODO-CT) that covered approximate polar and azimuthal angular ranges of 43° and 40° , respectively, in the laboratory. Each of these telescopes subtended a solid angle of 1.83 msr and consisted of a 300 μm thick silicon detector followed by a 6 cm thick CsI(Tl) scintillation detector. The centers of neighboring telescopes were separated by relative angles of 3.3° . To provide good coverage for light charged particles emitted at center-of-mass angles of $\theta_{\text{cm}} \approx 90^\circ$, where contributions from the decay of projectile-like and target-like fragments are minimal, the central angle of the hodoscope was placed at $58^\circ, 50.6^\circ, 42.7^\circ$, and 42.7° at incident energies of $E/A=35, 70, 100$ and 120 MeV, respectively. In addition, isotopically resolved fragments with $3 \leq Z \leq 6$ were detected with four heavy-ion telescopes constructed of planar 75 and 5000 μm thick silicon detectors located at polar angles of $\theta = 27^\circ, 36^\circ, 75^\circ$, and 84° . The silicon detectors were calibrated to an accuracy of 2% with a precision pulser and alpha particles emitted from a ^{238}Th source. The CsI(Tl) scintillators were calibrated to an accuracy of 3% with recoil protons elastically scattered from a CH_2 target by ^{86}Kr ions at $E/A=35$ MeV and ^4He ions at $E/A=22$ and 40 MeV. Figure 1 demonstrates the isotopic resolution achieved for elements up to carbon with the four heavy-ion telescopes.

The relative populations of widely separated states in emitted ^4He ($J_i^\pi = 0^+, E^* = 20.1$ MeV; $J_j^\pi = 0^+, \text{g.s.}$), ^5Li ($J_i^\pi = 3/2^+, E^* = 16.7$ MeV; $J_j^\pi = 3/2^-, \text{g.s.}$),

and ${}^8\text{Be}$ ($J_1^\pi = 1^+, E^* = 17.6 \text{ MeV}; J_j^\pi = 2^+, E^* = 3 \text{ MeV}$) fragments were measured with the 96 element hodoscope. Five of these six states are particle unstable; their populations were measured by detecting the coincident decay products. In Fig. 2, we present data at $E/A=100 \text{ MeV}$ for the decay of particle unstable ${}^5\text{Li}$ nuclei in the form of correlation functions, $R(E_{rel})$, which are defined in terms of the measured coincidence yield $Y_{12}(p_1, p_2)$ and the singles yield $Y_1(p_1)$ and $Y_2(p_2)$ as follows:

$$\Sigma Y_{12}(p_1, p_2) = C[1 + R(E_{rel})]\Sigma Y_1(p_1)Y_2(p_2). \quad (3)$$

Here, p_1 and p_2 are the momenta of the two particles in the laboratory and $E_{rel} = \frac{1}{2}\mu v_{rel}^2$ is the kinetic energy in the center-of-mass frame of the two particles. The sums on both sides of Eq. (3) are extended over all energy, position and detector combinations corresponding to a given bin of E_{rel} . The normalization constant C in Eq. (3) is chosen to normalize $1 + R(E_{rel})$ to unity at large E_{rel} where resonances are not observed in the exit channel.

The solid points in Fig. 2 correspond to the correlation functions measured using the previously described central collision gate. The d- ${}^3\text{He}$ correlation function in the upper panel of the figure displays a structure at low E_{rel} corresponding to the $J^\pi = 3/2^+, E^* = 16.7 \text{ MeV}$ excited state and the p- α correlation in the lower panel displays a broad structure at $E_{rel} \approx 2 \text{ MeV}$ corresponding to $J^\pi = 3/2^-$ ground state of ${}^5\text{Li}$. The coincidence yield in the correlation function was fitted by superimposing the resonant decay of ${}^5\text{Li}$ and a non-resonant contribution wherein the two measured coincident particles are emitted independently but interact by long range mutual Coulomb interactions as they propagate from the production region. The response of the experimental apparatus was folded into the calculations. The solid, dashed and dotted lines represent minimum and maximum background estimates from different assumption on the uncorrelated emission evaluated by model calculations. Both the full fit and the corresponding non-resonant background are separately shown.

Extracted values of $T_{\Delta E}$ are plotted as solid circles ($T_{\Delta E}({}^5\text{Li})$), solid diamonds ($T_{\Delta E}({}^4\text{He})$), and solid squares ($T_{\Delta E}({}^8\text{Be})$) in Figure 3 as a function of incident energy. The experimental uncertainties primarily reflect uncertainties in the subtraction of

the non-resonant background. The extracted temperatures $T_{\Delta E}$ are of the order of 4 MeV and show little variation with incident energy, a trend also observed for central Au+Au collisions [7,12].

Values of T_{iso} were obtained via Eq. (1) at the four incident energies. Carbon isotope yields were measured with the heavy-ion telescopes while the isotope yield ratios for lighter particles ($Z < 6$) were obtained with selected detectors in the hodoscope situated at $\theta_{cm} \approx 90^\circ \pm 10^\circ$. (Over the measured angular range, all the single isotope yield ratios are relatively constant with respect to scattering angle.) The experimental uncertainties in these ratios mainly reflected the uncertainties in the particle identification (up to 10% in ^{11}C). Values for $T_{iso}(C-Li)$ (open circles) obtained from ($^{6,7}\text{Li}$, $^{11,12}\text{C}$) isotope ratios vary little with incident energy, similar to the trends exhibited by the temperatures $T_{\Delta E}(^5\text{Li})$, $T_{\Delta E}(^4\text{He})$, and $T_{\Delta E}(^8\text{Be})$ extracted from excited states populations. Values of T_{iso} extracted from other possible ratios based upon the large binding energy difference of (^{11}C , ^{12}C) isotopes, including those obtained from ($^{12,13}\text{C}$, $^{11,12}\text{C}$), follow the same behavior as $T_{iso}(C-Li)$. In contrast, values of $T_{iso}(He-Li)$ (open diamonds) obtained from ($^{6,7}\text{Li}$, $^3,^4\text{He}$) isotopes increase monotonically with incident or excitation energy, consistent with trends recently reported for other systems [5, 9,12]. Similarly increasing trends are extracted from other possible ratios based upon the large binding energy difference between ^3He and ^4He isotopes.

Some corrections to the measured apparent temperatures can be expected due to the secondary decay of heavier isotopes that feed the yields used in Eqs. (1) and (2) [7,13,14]. Secondary decay calculations, however, predict the secondary decay corrections to $T_{\Delta E}(^5\text{Li})$, $T_{\Delta E}(^4\text{He})$, $T_{\Delta E}(^8\text{Be})$, and $T_{iso}(He-Li)$ to be relatively small for apparent temperatures of the order of 4.5 MeV [7]. Moreover, the secondary decay corrections to $T_{\Delta E}(^4\text{He})$ and $T_{iso}(He-Li)$ should be nearly identical for [31] at all source temperatures because B and ΔE are comparable and because both are affected primarily by the feeding contributions to the ground state yield of ^4He .

The use in Eqs. (1) and (2) of measured binding and excited state energies and the neglect of a dependence on the volume of the emitted particle, however, is a low density approximation [4,14,32]. In ref. [14], high values for $T_{iso}(He-Li)$ and low values for $T_{\Delta E}(^5Li)$ have been predicted within a common statistical framework by assuming that the radius of the unstable $T_{\Delta E}(^5Li)$ nuclei is equal to the sum of radii of its decay products [33] whereby excited 5Li nuclei are 3.1 times larger in volume than ground state 5Li nuclei. The yield of excited $^5Li^*$ is consequently suppressed due to the constraint that its size imposes upon the size of the remaining system. In contrast, the volume of $^8Be^*(17.6 \text{ MeV})$ is 0.95 times the volume of $^8Be^*(3 \text{ MeV})$. Since the radii of $^8Be^*(17.6 \text{ MeV})$ and $^8Be^*(3 \text{ MeV})$ [33] are nearly the same, $T_{\Delta E}(^8Be)$ should not be suppressed. The expected values for $T_{\Delta E}(^8Be)$ should therefore be much higher than the observed values for $T_{\Delta E}(^5Li)$ at high incident energies - an effect not observed experimentally. Thus the method described in ref. [14] to reconcile excited state and isotope temperatures is not supported by the present data.

The overall picture provided by the present data suggests that the temperatures deduced from the 3He yields are inconsistent with all other cases investigated for which $B \gg T$. This discrepancy may reflect differences in the emission environments of 3He as compared to the emission environments for fragments and alpha particles. Investigations of fragment-fragment correlations [34] and fragment charge distributions [34,35] have reported evidence for a hierarchy of timescales whereby light particle emission precedes fragment emission rendering the two processes out of equilibrium. Theoretical support for this picture is provided by the predictions of dynamic models for light particle emission and also by statistical emission rate approaches [28, 30]. The precise degree to which light particle emission during the early stages of the collision is further enhanced by statistical emission of predominantly light particles at very high initial temperature depends on the timescale for thermalization and requires further experimental and theoretical investigations. Qualitatively, however, both effects will cause a divergence of temperatures derived from poorly bound light particles such as d, t, 3He from those derived from strongly bound fragments observed in the present work.

In summary, populations of the states of ${}^4\text{He}$, ${}^5\text{Li}$, and ${}^8\text{Be}$ and double ratios constructed from the yields ${}^3,4\text{He}$, ${}^{6,7,8}\text{Li}$, ${}^{11,12,13}\text{C}$ isotopes were measured for central Kr+Nb collisions at $E/A=35\text{-}120$ MeV. These ratios were used to extract apparent temperatures for emission using Eqs. 1 and 2. Consistent and approximately constant apparent temperatures were obtained from the excited states of ${}^4\text{He}$, ${}^5\text{Li}$, and ${}^8\text{Be}$ nuclei and from the yields of carbon isotopes. In contrast, apparent temperatures obtained from ratios of helium isotopes increase monotonically with incident energy. This discrepancy may be consistent with a preference for ${}^3\text{He}$ emission during the early stages of the collision and enhanced fragment emission at a lower temperature during a later stage.

This work was supported by the National Science Foundation under Grant Nos. PHY-95-28844 and PHY-93-14131.

REFERENCES:

1. J.P. Bondorf, R. Donangelo, I.N. Mishustin, H. Schulz, Nucl. Phys. A **444**, 460 (1985).
D.H.E. Gross, Rep. Prog. Phys. **53**, 605 (1990).
2. W.G. Lynch, Ann. Rev. Nucl. and Part. Sci. **37**, 493 (1987) and refs. therein.
3. H. Jaqaman, A.Z. Mekjian, and L. Zamick, Phys. Rev. C **27**, 2782 (1983).
4. S. Albergo et al., Nuovo Cimento **89**, 1 (1985).
5. J. Pochodzalla et al., Phys. Rev. Lett. **75**, 1040 (1995).
6. M.B. Tsang, W.G. Lynch, H. Xi, W.A. Friedman, Phys. Rev. Lett. **78**, 3836 (1997).
7. M.J. Huang et. al., Phys. Rev. Lett. **78**, 1648 (1997).
8. R. Wada et al., Phys. Rev. C **55**, 227 (1997).
9. Y-G. Ma et. al, Phys. Lett. B, **B390**, 41 (1997)
10. H.F. Xi et al., Z. fur Physik **A 359** 397 (1997).
11. H. Xi, W.G. Lynch, M.B. Tsang, W.A. Friedman, Phys. Rev. C **54** R2163, (1996).
12. V. Serfling et al., GSI preprint, GSI98-06 (1998)
13. A. Kolomiets et al., Phys. Rev. C **54**, R472 (1996).
14. F. Gulminelli and D. Durand, Nucl. Phys. A **615**, 117 (1997).
15. J.B. Natowitz et al., Phys. Rev. C **52**, R2322 (1995)
16. C. B. Das, L. Satpathy, Phys. Rev. C **57**, R35 (1998)
P. F. Mastinu et al., Phys. Rev. C **57**, 831 (1998)
17. Z. Majka et al., Phys. Rev. C **55**, 2991 (1997)
J. N. De, S. Das Gupta, S. Shlomo and S.. Sammadar, Phys. Rev. C **55**, R1641 (1997)
S. J. Lee et al., Phys. Rev. C **56**, 2621 (1997)

- S. K. Samaddar, J. N. De, S. Shlomo, Phys. Rev. Lett. **79**, 4962 (1997).
18. W.C. Hsi et al., Phys. Rev. Lett. **73**, 3367 (1994).
S.C. Jeong et al., Phys. Rev. Lett. **72**, 3468 (1994).
 19. H.M. Xu et. al., Phys. Rev. C **40**, 186 (1989).
 20. T.K. Nayak et al., Phys. Rev. C **45**, 132 (1992).
 21. F. Zhu et al., Phys. Rev. C **52**, 784 (1995).
 22. J. Pochodzalla et al., Phys. Rev. C **35**, 1695 (1987).
Z. Chen et al., Phys. Rev. C **36**, 2297 (1987).
 23. C. Schwarz et. al. Phys. Rev. C **48**, 676 (1993).
 24. Xi Hongfei et al., Nucl. Phys. **A552**, 281 (1993).
 25. R. Wada et al., Phys. Rev. C **55**, 227 (1997)
 26. W. Benenson, D. J. Morrissey, and W. A. Friedman, Ann. Rev. Nucl. and Part. Sci. **44**, 27 (1994) and refs. therein.
 27. W.G. Friedman, Phys. Rev. C **42**, 667 (1990).
 28. R. Bougault et al., preprint, LPCC97-04 (1997).
 29. H. Xi et al., Phys. Rev. C, Phys. Rev. C **57**, R467 (1998).
 30. G.J. Kunde et al., Phys. Lett. **B416**, 56 (1998)
 31. H. Xi et al., MSU preprint MSUCL-1055 (1996).
 32. H. Bethe, Pethick, Nucl. Phys. **A175**, 225 (1971).
 33. H. De Vries, C.W. De. Jager and D. de Vries Atomic Data and Nuclear Data Table, **36**, 503 (1987).
 34. T. M. Hamilton, et al., Phys. Rev., C **53**, 2273 (1996);
E. W. Cornell, et al., Phys. Rev. Lett. **77**, 4508 (1996)
 35. C. Williams et al., Phys. Rev. C **55**, R2132 (1997).

FIGURE CAPTIONS:

Fig. 1: Typical particle identification spectra obtained from the heavy-ion telescopes. Isotopic resolution up to carbon and beyond is routinely obtained.

Fig. 2: Correlation functions, exhibiting the decay of ${}^5\text{Li}$ in its $E^*=16.7$ MeV excited state (top panel) and its ground state (bottom panel), as a function of relative energy of the decay products.

Fig. 3: Dependence of T_{iso} (open symbols) and $T_{\Delta E}$ (closed symbols) upon the incident energy.

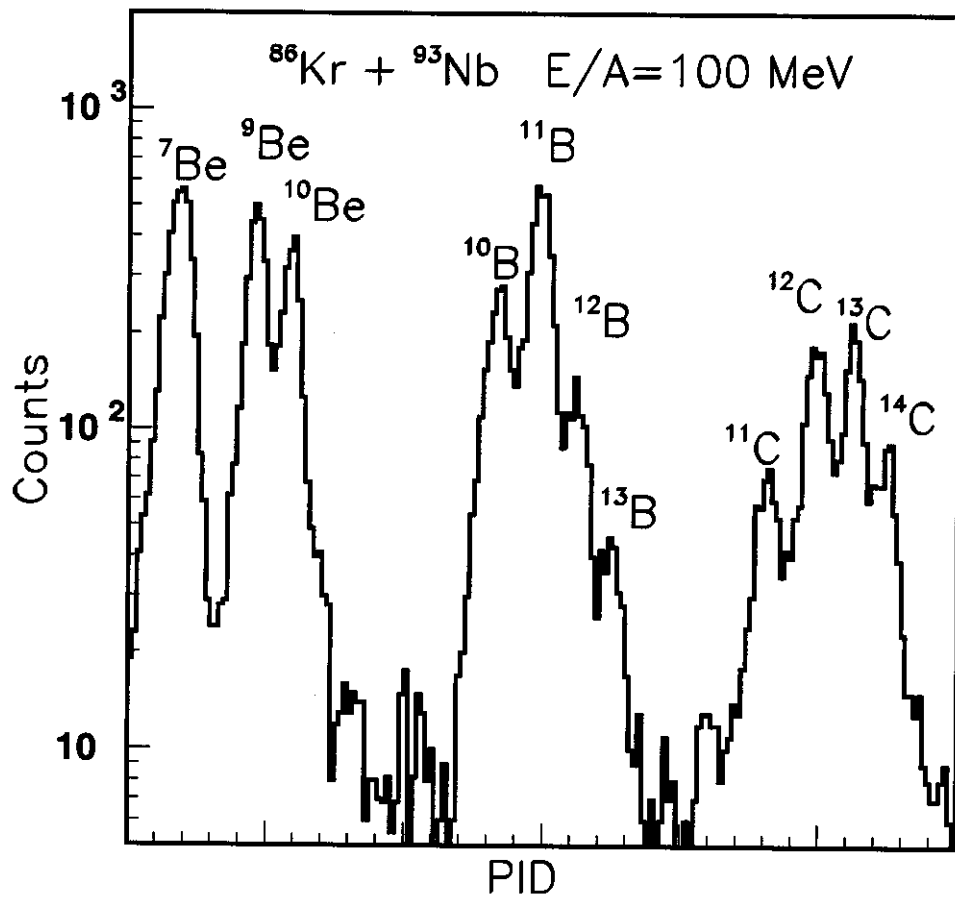


Fig.1

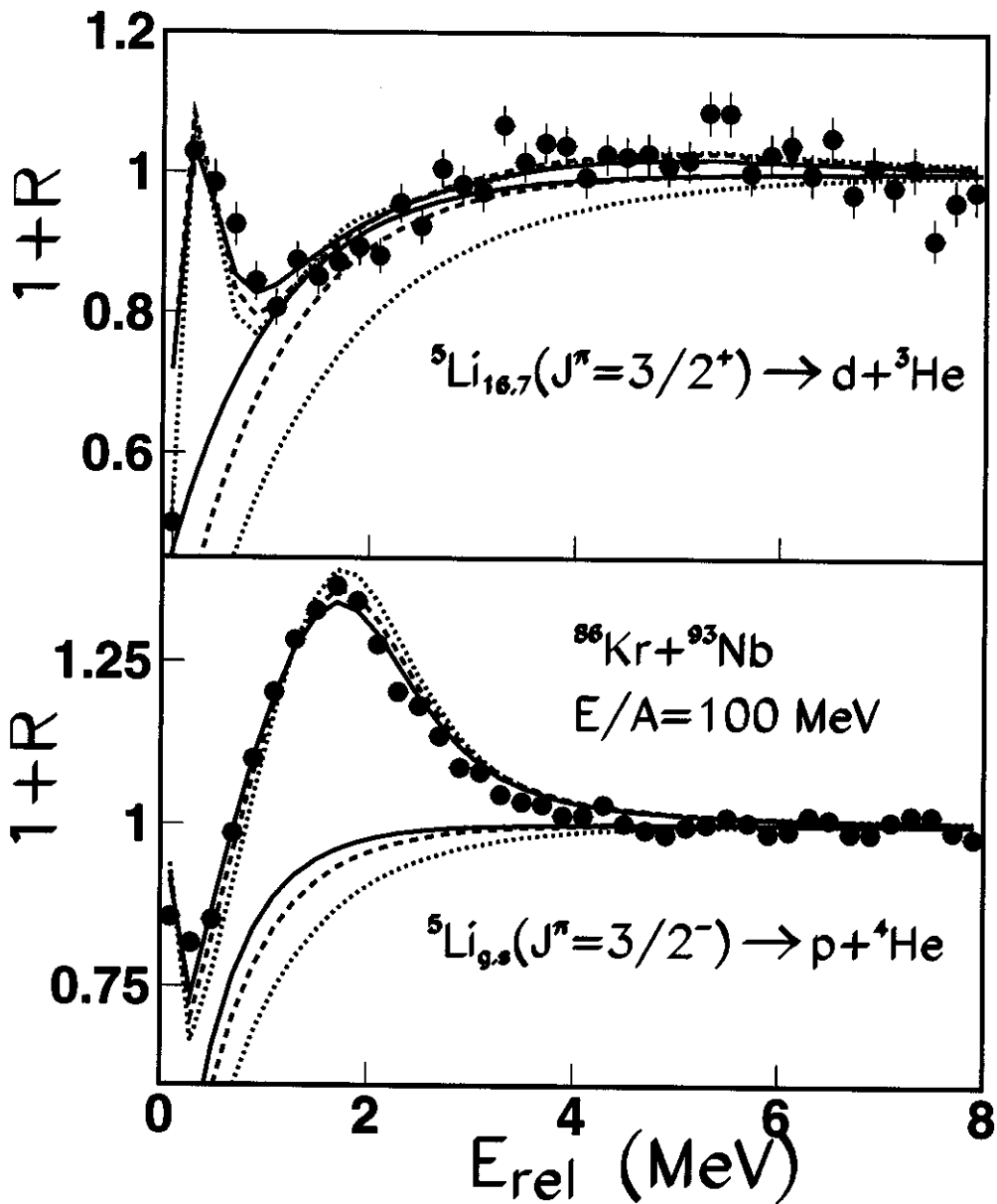


Fig. 2

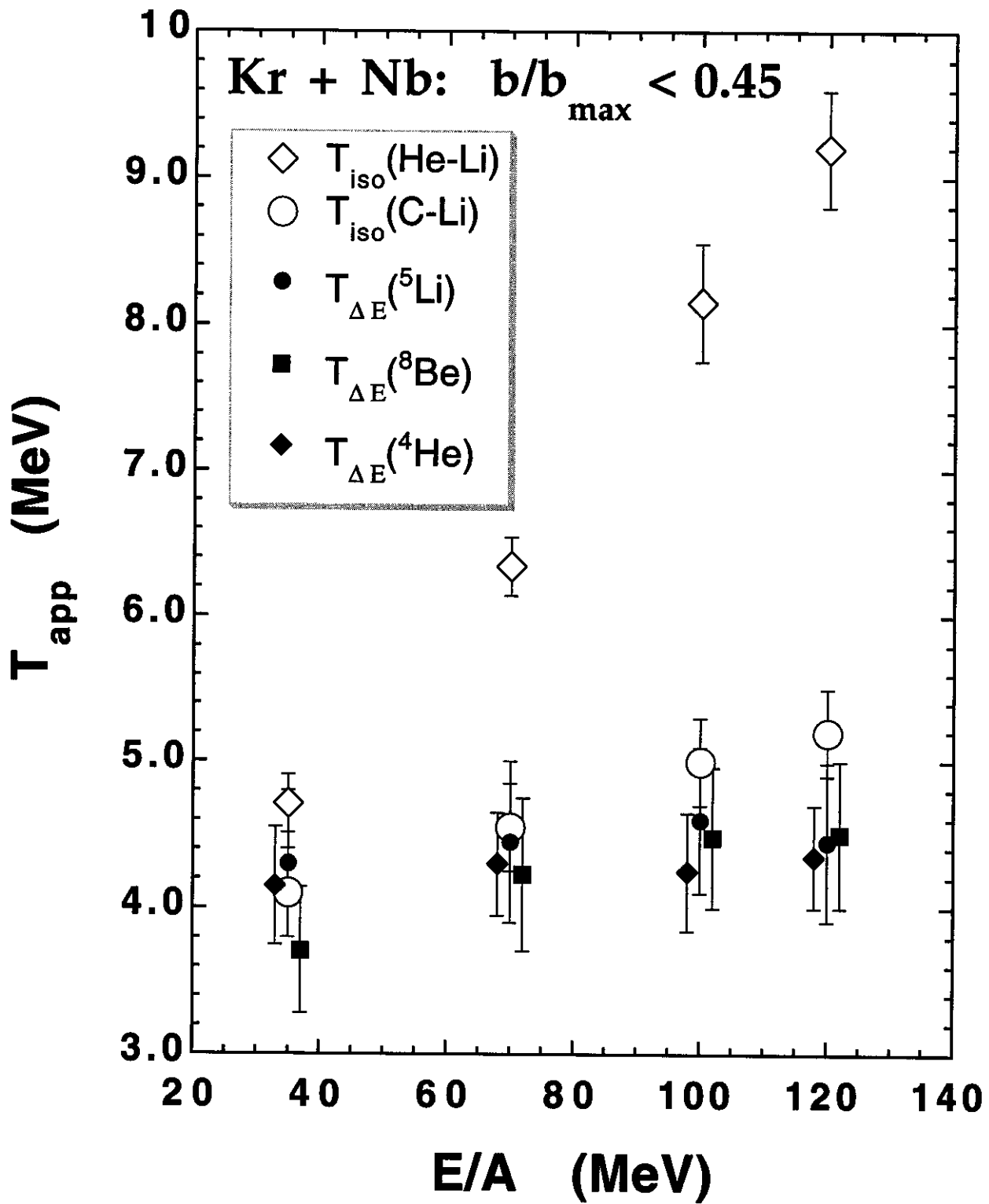


Fig.3